MATHEMATICAL MODELING AND COMPUTING, Vol. 12, No. 3, pp. 709–723 (2025)

Flood frequency analysis of daily water levels using the L-moment and TL-moment approaches at river stations in Pahang

Arba F. A. N.[1], Azahar A. A.[1,*], Marsani M. F.[1], Kasihmuddin M. S. M.[1], Someetheram V.[1], Mansor M. A.[2], Jan N. A. M.[3], Jamaludin S. Z. M.[1]

[1] *School of Mathematical Sciences, Universiti Sains Malaysia, 11800 USM, Penang, Malaysia*
[2] *School of Distance Education, Universiti Sains Malaysia, 11800 USM, Penang, Malaysia*
[3] *Department of Physical and Mathematical Science, Faculty of Science, Universiti Tunku Abdul Rahman, Kampar Campus, 31900 Kampar, Perak, Malaysia*
[*] *Corresponding author: adilaazahar@usm.my*

(Received 17 December 2024; Revised 7 April 2025; Accepted 5 May 2025)

The application of flood frequency analysis is essential for understanding and managing the risks associated with extreme water level events. This study examines the Pahang River basin, specifically focusing on water levels at Sungai Pahang (Temerloh) and Sungai Lipis (Benta). Probability distributions and return period concepts are applied to assess flood occurrences. The study has two main objectives: first, to determine the most suitable probability distribution for modeling flood events among the Generalized Extreme Value (GEV), Generalized Logistic (GLO), and Generalized Pareto (GPA) distributions, using both L-moments and TL-moments for parameter estimation; and second, to estimate expected water levels for return periods of 2, 5, 10, 50, and 100 years using the identified best-fit distributions. The study employs the Mean Absolute Deviation Index (MADI) and Ratio Diagram tools to evaluate distribution performance to achieve these objectives. The results indicate that the GLO distribution, estimated using TL-moments (1;0), provides the best fit for the water level data. The findings suggest that water levels in Sungai Pahang and Sungai Lipis will likely exceed the critical danger thresholds of 33 meters and 75 meters within the next 5 and 10 years, respectively, highlighting the need for proactive flood management strategies.

Keywords: *flood frequency analysis; L-moments; TL-moments; generalized logistic distribution; return period; Pahang river basin.*

2010 MSC: 62P12, 60G70, 86A05 **DOI:** 10.23939/mmc2025.03.709

1. Introduction

Malaysia is a tropical climate country that experiences heavy rainfall during monsoon seasons, particularly between April and September (Southwest Monsoon) and between October and March (Northeast Monsoon). As a result, flooding is a recurring problem in some areas of Malaysia, particularly in the East Coast states of Kelantan, Terengganu, and Pahang, as well as in parts of Sabah and Sarawak. Because of their terrain, which includes large river basins and flood-prone shorelines, these areas are prone to floods. While flooding in Malaysia can be attributed to natural factors such as heavy rainfall, drastic increase in river flows, and topography [1], human activities have also contributed to the frequency and intensity of floods. Deforestation due to logging and land clearance can reduce the forested region‘s ability to absorb and store rainfall, resulting in increased runoff and flooding downstream. Additionally, inappropriate land use practices such as construction in flood-prone areas can exacerbate the impact of floods, resulting in increased property damage and loss of life [2–5]. The consequences of floods can be devastating for both people and the environment. Floods can cause casualties, property

This work was supported by Ministry of Higher Education Malaysia for Fundamental Research Grant Scheme with Project Code: FRGS/1/2022/STG06/USM/03/1.

destruction, and economic turmoil [6]. To mitigate the impact of floods, it is crucial to have accurate and dependable flood frequency analyses that estimate the likelihood of floods of various magnitudes and frequencies [7–9].

Recently, considerable literature has emerged, focusing on extreme value theory, particularly emphasizing the application and performance of various statistical methods in analyzing extreme events. Among these, TL moments have rapidly become a key instrument in enhancing the precision and robustness of parameter estimation for extreme value distributions. It is now well established from a variety of studies that TL moment estimation provides valuable insights into the tail behavior of distributions, offering a more nuanced understanding of extreme event modeling. This approach has proven effective in addressing challenges associated with traditional methods, especially in complex scenarios where conventional techniques may fall short. It has been noted that the Generalized Extreme Value (GEV) distribution, which encompasses a wide range of extreme value behaviors, often benefits from advanced estimation techniques to accurately capture the tail characteristics. Recent advancements have demonstrated that TL moments can significantly improve the estimation process by offering enhanced robustness and accuracy [8, 10].

Similarly, recent studies have established that the Generalized Logistic (GLO) distribution, known for its versatility in modelling extreme values [11], also stands to gain from incorporating TL moment estimation [12]. The integration of TL moments in GLO distributions can lead to more reliable and precise parameter estimates, particularly in contexts where traditional methods may struggle with data irregularities or outliers. Although studies have recognized the potential of GEV and GLO distributions, there has been little discussion about the application and advantages of TL moment estimation in these contexts. Addressing this gap, our research aims to explore how TL moments can be effectively employed to refine the estimation of parameters for both GEV and GLO distributions, thereby advancing the field of extreme value analysis [13–19].

This study aims to contribute to the understanding of flood frequency in Pahang by focusing on two river stations, Sungai Pahang in Temerloh and Sungai Lipis in Benta, which have not been thoroughly investigated in terms of flood frequency analysis. By utilizing daily water level data and comparing different distribution functions, the study aims to provide a more comprehensive understanding of flood frequency, particularly in catastrophic flood occurrences. There are two specific objectives for this study. First, to identify the best probability distribution among generalized extreme value (GEV), generalized logistic (GLO), and generalized pareto (GPA), using L-moment, and TL-moment parameter estimation methods for daily water level data for the two river stations. Secondly, to evaluate the expected water level based on the concept of return period using the distributions identified as the best fit. To achieve these objectives, secondary data of water level for both river stations, spanning the period from 1965 to 2009 was obtained from the Department of Irrigation and Drainage Malaysia. R programming software will be used to estimate the parameter values of the probability distribution, and the concept of return period will be applied to evaluate the expected water level using the identified best fit distributions for both stations. Overall, this study aims to contribute to the existing literature on flood frequency analysis in Pahang and inform future flood mitigation efforts in the area. By providing a more comprehensive understanding of flood patterns and risks, this study has the potential to improve flood risk management and reduce the impact of floods on communities and the environment.

2. Methodology

Parameter estimations were done to the water level data of the two river stations using L-moment and TL-moment $(1, 2, 3, 4; 0)$ parameter estimation methods for three probability distributions of interest which are the GEV, GLO, and GPA. These distributions will then be tested using the Kolmogorov–Smirnov (KS) test to determine whether they fit the data well. To select the best-fitting distribution for the river station data, MADI and ratio diagram were done. Evaluation was also done where the datasets are first partitioned into two sets: training and testing. These partitions underwent the same parameter estimation procedure, and all distributions were compared using MADI. The distribution with the lowest MADI for the testing set was considered as the best-fit distribution for the dataset of water level for the two river stations. Once the best distribution was determined, future water level values for the next 2, 5, 10, 50, and 100 years were evaluated using the concept of return period.

2.1. Probability distributions

According to [20], frequency analysis is the evaluation of how frequent a specific occurrence will occur. Flood estimation over long time periods can often be necessary in engineering and structural design. However, one of the primary issues is the selection of an appropriate probability model, as there are no unambiguous opinions on which distribution should be applied to frequency analysis [21]. In this study, three probability distributions are used to analyse the data. Understanding the probability distribution allows for evaluating flood occurrence.

Generalized extreme value (GEV). Generalized extreme value (GEV) is commonly used in fields dealing with extreme values such as air pollution, operational risk management, finance, economics, hydrology and many others [22]. The three parameters in the distribution are location (ξ), scale (α), and shape (k). Meanwhile, x refers to the water level in metres (m) for both river stations. The probability distribution function (pdf) and cumulative distribution function (cdf) as proposed by [23] are given by Equations (1) and (2)

$$f(x) = \frac{1}{\alpha}\left[1 - k\left(\frac{x-\xi}{\alpha}\right)\right]^{\frac{1}{k}-1} e^{-\left[1-k\left(\frac{x-\xi}{\alpha}\right)\right]^{\frac{1}{k}}}, \tag{1}$$

$$F(x) = e^{-\left[1-k\left(\frac{x-\xi}{\alpha}\right)\right]^{\frac{1}{k}}}. \tag{2}$$

According to [24], the sign for parameter k determines the range of variable x. Variable x can have a range of $\xi + \frac{\alpha}{k} < x < \infty$ when parameter k is negative, which is ideal for flood frequency analysis. From the cdf, the inverse function or quantile function $x(F)$ for GEV is given by Equation (3),

$$x(F) = \xi + \frac{\alpha}{k}\left[1 - (1 - \ln F)^k\right]. \tag{3}$$

Generalized logistic (GLO). The generalized logistic (GLO) distribution is a versatile probability distribution that can take on a variety of shapes, including symmetric, skewed, and heavy-tailed distributions. The three parameters that define this distribution are location (ξ), scale (α), and shape (k). Meanwhile, x refers to the water level in metres (m) for both river stations. The pdf and cdf as proposed by [23] are as shown in Equations (4) and (5),

$$f(x) = \frac{1}{\alpha}\left[1 - k\left(\frac{x-\xi}{\alpha}\right)\right]^{\frac{1}{k}-1}\left[1 + \left[1 - k\left(\frac{x-\xi}{\alpha}\right)\right]^{\frac{1}{k}}\right]^{-2}, \tag{4}$$

$$F(x) = \left[1 + \left[1 - k\left(\frac{x-\xi}{\alpha}\right)\right]^{\frac{1}{k}}\right]^{-1}. \tag{5}$$

Similar to GEV, the range of x for the generalized logistic distribution depends on the shape parameter, k [24]. It has a range of $-\infty < x < \xi + \frac{\alpha}{k}$ when $k > 0$, and $-\infty < x < \infty$ when $k = 0$. Furthermore, the range of x can be $\xi + \frac{\alpha}{k} \leqslant x \leqslant \infty$ when $k < 0$. The author also added that the distribution is considered as the logistic distribution when the shape parameter, $k = 0$. From the cdf, equation (6) is the inverse function or quantile function, $x(F)$ for GLO,

$$x(F) = \xi + \frac{\alpha}{k}\left[1 - \left(\frac{[1-F]}{F}\right)^k\right]. \tag{6}$$

Generalized Pareto (GPA). Another distribution used in modelling extreme values is the generalized pareto (GPA) [23]. Like GEV and GLO, this distribution also has three parameters which are location (ξ), scale (α), and shape (k). Meanwhile, x refers to the water level in metres (m) for both river stations. Based on [24] there are two special cases for this distribution. It is considered as an exponential distribution when $k = 0$ and when $k = 1$, this distribution is the uniform distribution having the interval $\xi \leqslant x \leqslant \xi + \alpha$. The probability distribution function (pdf) for GPA is given by equation (7) and equation (8),

$$f(x) = \frac{1}{\alpha}\left[1 - k\frac{x-\xi}{\alpha}\right]^{\frac{1}{k}-1}, \tag{7}$$

$$F(x) = 1 - \left[1 - k\frac{x-\xi}{\alpha}\right]^{\frac{1}{k}}. \tag{8}$$

The range of x, similar to the previous distributions are dependent on the shape parameter, k. The range of x is $\xi \leqslant x \leqslant \xi + \frac{\alpha}{k}$ for $k > 0$ and $\xi \leqslant x < \infty$ for $k \leqslant 0$. From the cdf, equation (9) is the inverse function or quantile function, $x(F)$ for GPA,

$$x(F) = \xi + \frac{\alpha}{k}\left[1 - (1-F)^k\right]. \tag{9}$$

2.2. Parameter estimations

Many approaches have been utilized by researchers in Flood Frequency Analysis studies to fit chosen statistical distributions to flood series data. L-moment introduced by [24] has been widely utilized in hydrology, meteorology, and other areas to analyse extreme events, especially when traditional moments may not be suitable or useful. Reference [25] has proposed an alternative version of the L-moment known as the Trimmed L-moment (TL-moment).

L-moment. L-moment is a statistical measurement used to estimate probability distribution characteristics. It was introduced as an alternative to the traditional method of utilising raw data. According to [24], L-moment estimates distribution parameters using linear combinations of order of statistics which provides reliability and efficiency, especially for heavy-tailed distributions. L-moment has been used in various fields such as hydrology, quality control, engineering, and meteorology [25]. L-moment has arisen from the modification of probability weighted moments (PWM). The theory of PWM has been summarized and defined in Equation (10),

$$\beta_r = \int_0^1 x(F)\, F^r \, dF, \tag{10}$$

where β_r is the r^{th} order of PWM, $F(x)$ is the CDF for x, $x(F)$ is the inverse of cdf of x, and $r = 0, 1, 2, \ldots$ is a non-negative integer. L-moment defined in equation (11) and equation (12),

$$\lambda_{r+1} = \sum_{k=0}^{r} p_{r,k}\beta_k, \quad k = 0, 1, 2, \ldots, r, \tag{11}$$

where

$$p^*_{r,k} = (-1)^{r-k}\binom{r}{k}\binom{r+k}{k}, \quad r = 0, 1, 2, \ldots. \tag{12}$$

The first L-moment, λ_1 is defined as the mean of the distribution and the second L-moment, λ_2 is the dispersion or the measure of scale. Meanwhile, the third, λ_3 and fourth, λ_4 L-moment are the skewness and kurtosis respectively. From the L-moment, the first four are listed in Equation (13),

$$\begin{aligned} &\lambda_1 = \beta_0, \\ &\lambda_2 = 2\beta_1 - \beta_0, \\ &\lambda_3 = 6\beta_2 - 6\beta_1 + \beta_0, \\ &\lambda_4 = 20\beta_3 - 30\beta_2 + 12\beta_1 - \beta_0. \end{aligned} \tag{13}$$

These formulations can be further simplified using expected values of order statistics. Let $X_1, X_2, \ldots, X_r$ be a conceptual random sample of size r with quantile function, $Q(F) = X(F)$ from a continuous distribution, and $X_{1:r} \leqslant X_{2:r} \leqslant \ldots \leqslant X_{r:r}$ denote the corresponding order statistics.

The $r_t h$ L-moment defined in Equation (14),

$$\lambda_r = \frac{1}{r}\sum_{k=0}^{r-1}(-1)^k\binom{r-1}{k}E[X_{r-k:r}], \quad r = 1, 2, \ldots, \tag{14}$$

where r refers to the order of the L-moment while $E[X_{r-k:r}]$ refers to the expected values of the $r-k$ order statistics of a sample size r. Based on [20], the expectation of an order statistics is below equation (15),

$$E[X_{i:r}] = \frac{r!}{(i-1)!(r-i)!} \int_0^1 x(F)\, F^{i-1} (1-F)^{r-i}\, dF. \tag{15}$$

This leads to the L-moment probability distribution to become as in equation (16),

$$\begin{aligned} \lambda_1 &= E[X_{1:1}], \\ \lambda_2 &= \frac{1}{2} E[X_{2:2} - X_{1:2}], \\ \lambda_3 &= \frac{1}{3} E[X_{3:3} - 2X_{2:3} + X_{1:3}], \\ \lambda_2 &= \frac{1}{4} E[X_{4:4} - 3X_{3:4} + 3X_{2:4} - X_{1:4}]. \end{aligned} \tag{16}$$

L-moment ratio τ_2, τ_3 and τ_4 are the Coefficient of L-variation (L-CV), L-Skewness and L-Kurtosis respectively are calculated as follows equation (17),

$$\tau_2 = \frac{\lambda_2}{\lambda_1}, \quad \tau_3 = \frac{\lambda_3}{\lambda_2}, \quad \tau_4 = \frac{\lambda_4}{\lambda_3}. \tag{17}$$

The sample L-moment can be written in (18),

$$l_{r+1} = \sum_{i=0}^{r} (-1)^{r-1} \binom{r}{i} \binom{r+i}{i} b_i, \quad r = 0, 1, 2, \ldots, n-1, \tag{18}$$

where b refers to the unbiased estimator for β. And the first four sample L-moment estimates are below equation (19),

$$\begin{aligned} l_1 &= b_0, \\ l_2 &= 2b_1 - b_0, \\ l_3 &= 6b_2 - 6b_1 + b_0, \\ l_4 &= 20b_3 - 30b_2 + 12b_1 - b_0. \end{aligned} \tag{19}$$

In summary, the parameter estimation using L-moment for each distribution are as in Table 1.

Table 1. Parameter settings of the methods.

Distribution	Parameter estimation
GEV	$\xi = l_1 + \frac{\alpha}{k}[1 - \Gamma(1+k)]$ $\alpha = \frac{l_2 k}{\Gamma(1+k)(1-2^{-k})}$ $k = 785890c + 2.9554c^2$, where $c = \frac{2}{3+\tau_3} - \frac{\ln 2}{\ln 3}$
GLO	$\xi = l_1 - \alpha\left[\frac{1}{k} - \frac{\pi}{\sin k\pi}\right]$ $\alpha = \frac{l_2 \sin k\pi}{k\pi}$ $k = -\tau_3$
GPA	$\xi = l_1 - l_2(2+k)$ $\alpha = l_2[(k+1)(k+2)]$ $k = \frac{1-3\tau_3}{1+\tau_3}$

TL-moment. Due to L-moment being sensitive to outliers, where extreme values in the data affect it, particularly L-moment L3 and L4, which are used to evaluate skewness and kurtosis. Reference [25] has proposed an alternative version of the L-moment known as the Trimmed L-moment (TL-moment). In TL-moment the $E[X_{r-k:r}]$ is replaced by $E[X_{r+t_1-k:r+t_1+t_2}]$ for each r, where t_1 is the smallest trim and t_2 is the largest trim of the data. They have defined $r_t h$ TL-moment as in Equation (20),

$$\lambda_r^{(t_1;t_2)} = \frac{1}{r} \sum_{k=0}^{r-1} (-1)^k \binom{r-1}{k} E[X_{r+t_1-k:r+t_1+t_2}], \quad r = 1, 2, \ldots. \tag{20}$$

In TL-moment the $E[X_{r-k:r}]$ is replaced by $E[X_{r+t_1-k:r+t_1+t_2}]$ for each r, where t_1 is the smallest trim and t_2 is the largest trim of the data. They have defined r_{th} TL-moment as in Equation (21),

$$\lambda_r^{(t_1;t_2)} = \frac{1}{r}\sum_{k=0}^{r-1}(-1)^k\binom{r-1}{k}E[X_{r+t_1-k:r+t_1+t_2}], \quad r = 1, 2, \ldots. \tag{21}$$

Meanwhile, the TL-CV, $\tau_2^{(t_1,0)}$ TL-Skewness, $\tau_3^{(t_1,0)}$ and TL-Kurtosis, $\tau_4^{(t_1,0)}$ are calculated as in (22),

$$\tau_2^{(t_1;0)} = \frac{\lambda_2^{(t_1;0)}}{\lambda_1^{(t_1;0)}}\tau_3^{(t_1;0)} = \frac{\lambda_3^{(t_1;0)}}{\lambda_2^{(t_1;0)}}\tau_4^{(t_1;0)} = \frac{\lambda_4^{(t_1;0)}}{\lambda_2^{(t_1;0)}}. \tag{22}$$

The sample TL-moment is given in Equation (23),

$$l_r^{(t_1;0)} = \frac{1}{r\binom{n}{r+t_1+0}}\sum_{i=t_1+1}^{n}\sum_{k=0}^{r-1}(-1)^k\binom{r-1}{k}\binom{i-1}{r+t_1-k-1}\binom{n-i}{k}X_{i:n}. \tag{23}$$

Hence, the first four sample TL-moment $(t_1, 0)$ can be acquire as in equation (24),

$$\begin{aligned}
l_1^{(t_1;0)} &= \frac{1}{\binom{n}{1+t_1}}\sum_{i=t_1+1}^{n}\sum_{k=0}^{0}\binom{i-1}{t_1}\binom{n-i}{0}X_{i:n},\\
l_2^{(t_1;0)} &= \frac{1}{2\binom{n}{1+t_1}}\sum_{i=t_1+1}^{n}\sum_{k=0}^{1}(-1)^k\binom{1}{k}\binom{i-1}{1+t_1-k}\binom{n-i}{0}X_{i:n},\\
l_3^{(t_1;0)} &= \frac{1}{3\binom{n}{2+t_1}}\sum_{i=t_1+1}^{n}\sum_{k=0}^{2}(-1)^k\binom{2}{k}\binom{i-1}{2+t_1-k}\binom{n-i}{0}X_{i:n},\\
l_4^{(t_1;0)} &= \frac{1}{3\binom{n}{3+t_1}}\sum_{i=t_1+1}^{n}\sum_{k=0}^{3}(-1)^k\binom{3}{k}\binom{i-1}{3+t_1-k}\binom{n-i}{0}X_{i:n}.
\end{aligned} \tag{24}$$

For this study, TL-moment ($t_1 = 1, 2, 3, 4$; $t_2 = 0$) were used. The step for parameter estimation is the same for each TL-moment. By substituting the three distributions, GEV, GLO, and GPA into Equation (27) 27 and Equation (28), the summary for parameter estimation using TL-moment $(1, 2, 3, 4; 0)$ can be seen in Table 2.

Table 2. Parameter settings of the methods.

Distribution	Parameter estimation
GEV	$\xi = l_1^{(t_1;0)} + \frac{\alpha}{k}\left[1-\Gamma(1+k)\left(\frac{3}{2^k}-\frac{2}{3^k}\right)\right]$ $\alpha = \frac{l_2^{(t_1;0)}}{\Gamma(1+k)(1-2^{-k})}$ $k = 0.2816 - 2.8825\tau_3^{(t_1;0)} + 1.3744\left[\tau_3^{(t_1;0)}\right]^2 - 0.8462\left[\tau_3^{(t_1;0)}\right]^3$
GLO	$\xi = l_1 + \frac{l_2-\alpha}{k}$ $\alpha = \frac{2l_2^{(t_1;0)}\sin k\pi}{k\pi(k^2-1)}$ $k = -\frac{9\tau_3^{(t_1;0)}}{5}$
GPA	$\xi = l_1 + l_2(k+2)$ $\alpha = l_2[(k+1)(k+2)]$ $k = \frac{10-45\tau_3^{(t_1;0)}}{10+9\tau_3^{(t_1;0)}}$

Goodness of fit. Kolmogorov–Smirnov (KS) will be used in this study to determine whether the two datasets of daily water levels from the two river stations follow the three-parameter distributions: GEV, GLO, and GPA. The Kolmogorov–Smirnov test, developed by [26], is a non-parametric statistical test used to determine whether a dataset follows a specific probability distribution. The null hypothesis, H_0, for this test states that the dataset follows the specified probability distribution, whereas the alternative hypothesis, H_1, suggests otherwise. The test statistic, denoted as D_N, is calculated as the largest absolute difference between the empirical cumulative distribution function (ECDF), $F_N(x)$, of the daily water level dataset from the two river stations and the cumulative distribution function (CDF) of the hypothesized distribution, $F_0(x)$, given in equation (25),

$$D_N = \max |F_N(x) - F_0(x)|. \tag{25}$$

This test is one of the tests frequently used in the hydrological fields with the intention to examine the appropriateness of the distribution to the data. p-values associated with the test statistics, D_N were used to be compared with a significance level chosen for this study, $\alpha = 0.05$. The null hypothesis is rejected if the p-values are less than the significance level, α. The distribution does not fit the dataset if the null hypothesis is rejected.

Comparison of probability distribution. The goal of Mean Absolute Deviation Index (MADI) was to determine whether a particular distribution fits the data sufficiently well and to select the best fit to the data from a set of candidate distributions [26]. MADI was calculated as in equation (26),

$$\text{MADI} = \frac{1}{n}\sum_{i=1}^{n}\left|\frac{x_i - \hat{x_i}}{x_i}\right|, \tag{26}$$

where n is the number of observations for the river station, x_i is the observed water level value, while $\hat{x_i}$ is the predicted wate level value for the dataset. A distribution is better fit the actual data as compared to the other, when the value of MADI is smallest. One other method in determining the best distribution that fit the actual data is by using L-moment Ratio Diagram (LMRD) and TL-moment Ratio Diagram (TLMRD). These diagrams show which distributions are likely to provide an accurate fit to a set of data samples. The distribution closest to the positions of the sample L-moment and TL-moment ratios is considered the greatest fit to the actual data, while the distribution farthest away is considered the least suitable to reflect the data.

Evaluation procedure. To help choose the best appropriate probability distribution, evaluation by partitioning the datasets into two sets, training and testing of the two river stations were done. The probability distributions are first trained using the training set and data from the testing set was used to gather a better accuracy of the resulting distribution. Previous studies have shown that the best results are obtained when using 70% to 30% of data for training and the remaining for testing [27–29]. For this study, both datasets were partitioned into 70% training set and 30% testing set. After partitioning, parameter estimations of the three probability distributions, GEV, GLO, and GPA using L-moment and TL-moment $(1, 2, 3, 4; 0)$ were done to both training and testing set for the two river stations. The criterion for selection is determined by comparing their respective error measures by utilizing MADI. The best model is chosen when it has the least value of MADI.

2.3. The concept of return period

Extreme flood values do not adhere to a predictable pattern in terms of time and magnitude. According to [30], the definition of return period is the average length of time between floods events. Even though probability is not mentioned in the definition of return period, there is some justification for a correlation between the probability of occurrence of a flood event and its returning period. Return period is the probability of a flood to occur with a magnitude Q_T that may exceed a specific magnitude q, at least once for every T years. The probability of exceedance is given in equation (27),

$$P(Q_T \geqslant q) = \frac{1}{T}. \tag{27}$$

The cumulative probability of non-exceedance, $F(Q_T)$ represents the cumulative probability of a flood event with return period T not exceeding a specific magnitude q. This is denoted in equation (28),

$$F(Q_T) = P(Q_T \leqslant q) = 1 - P(Q_T \geqslant q) = 1 - \frac{1}{T}, \tag{28}$$

where (28) serves as the basis for estimating the magnitude of flood event, Q_T with a return period of T years. By substituting this equation into probability distribution function, the magnitude of flood event, Q_T can be solved. After the computation of parameters for the probability distribution,

Table 3. Quantile estimates for probability distribution.

Distributions	Quantiles estimates
GEV	$\xi + \frac{\hat{\alpha}}{\hat{k}}\left[1 - (-\log[1 - \frac{1}{T}])^{\hat{k}}\right]$
GLO	$\xi + \frac{\hat{\alpha}}{\hat{k}}\left[1 - (T-1)^{-\hat{k}}\right]$
GPA	$\xi + \frac{\hat{\alpha}}{\hat{k}}\left[1 - T^{-\hat{k}}\right]$

quantile estimates (x_T) from equations (3), (6) and (9) that correspond to various return periods can be evaluated. The F in the quantile estimates, x_T is substitute as $1 - \frac{1}{T}$ based on equation (28). The quantile estimates for the chosen probability distributions for this study which are GEV, GLO, and GPA in Table 3.

3. Findings and analysis

3.1. Descriptive statistics

Table 4. Quantile estimates for probability distribution.

Statistics	Sungai Pahang, Temerloh	Sungai Lipis, Benta
Mean	25.5768 m	71.1770 m
Standard Deviation	1.2657	0.9156
Skewness	1.8358	0.3748
Kurtosis	9.2948	4.5756

Both river stations were having distribution that is heavier on the right tail as compared to the left. This was further supported with the skewness values being 1.8358 and 0.3748, which indicated that the data were positively skewed. In addition, the kurtosis values of 9.2948 and 4.5756 indicated that the distributions have heavier tails and is more peaked than a normal distribution [31].

3.2. Parameter estimations

The parameters estimated for GEV, GLO, and GPA with their estimation methods are as shown in Tables 5 and 6 below.

Table 5. Parameters estimated for Sungai Pahang, Temerloh.

Distributions and Estimation Methods	Location	Scale	Shape
GEV L-moment	25.0036	0.8619	-0.082
GLO L-moment	25.344	0.5962	-0.2237
GPA L-moment	24.106	1.866	0.2688
GEV TL-moment (1;0)	25.01	0.831	-0.1043
GLO TL-moment (1;0)	25.3487	0.6121	-0.2068
GPA TL-moment (1;0)	24.3458	1.3681	0.0783
GEV TL-moment (2;0)	25.018	0.8154	-0.1137
GLO TL-moment (2;0)	25.3451	0.6277	-0.194
GPA TL-moment (2;0)	24.4659	1.1902	0.0094
GEV TL-moment (3;0)	25.0293	0.7997	-0.1222
GLO TL-moment (3;0)	25.3403	0.6366	-0.1877
GPA TL-moment (3;0)	24.5516	1.0867	-0.0301
GEV TL-moment (4;0)	25.0415	0.786	-0.1291
GLO TL-moment (4;0)	25.3362	0.6421	-0.1843
GPA TL-moment (4;0)	24.617	1.0185	-0.0559

The null hypotheses for all tests are defined as the distributions are fit for dataset of daily water level for each river stations. It should be rejected if the p-value is less than the significance level, α of 0.05. From Table 6, for Sungai Pahang, it turned out that the Generalized Pareto (GPA) distribution for both parameter estimation methods (L-moment and TL-moment $(1,2,3,4;0)$) were not suitable for the Sungai Pahang, Temerloh dataset since they have p-values that are less than $\alpha = 0.05$, which means the rejection of null hypotheses occurred. Meanwhile, for Sungai Lipis, Benta, it was found that the Generalized Pareto (GPA) with L-moment and TL-moment $(1;0)$ were not fit for the data since p-values are less than significance value, $\alpha = 0.05$. These probability distributions should not be used for further analysis. All other probability distributions have p-values that are greater than

Table 6. Parameters Estimated for Sungai Lipis, Benta.

Distributions and Estimation Methods	Location	Scale	Shape
GEV L-moment	70.8642	0.8891	0.2842
GLO L-moment	71.1772	0.5034	0.0003
GPA L-moment	69.6662	3.0231	1.001
GEV TL-moment (1;0)	70.8702	0.7973	0.1884
GLO TL-moment (1;0)	71.1791	0.5064	0.0062
GPA TL-moment (1;0)	70.1266	1.683	0.514
GEV TL-moment (2;0)	70.9195	0.6701	0.0809
GLO TL-moment (2;0)	71.182	0.4724	-0.0391
GPA TL-moment (2;0)	70.4274	1.1114	0.2646
GEV TL-moment (3;0)	70.9761	0.5774	0.0067
GLO TL-moment (3;0)	71.1976	0.4364	-0.0797
GPA TL-moment (3;0)	70.6158	0.8412	0.1279
GEV TL-moment (4;0)	71.0197	0.5221	-0.037
GLO TL-moment (4;0)	71.2135	0.4124	-0.1046
GPA TL-moment (4;0)	70.7305	0.7061	0.0525

Table 7. P-Values for Kolmogorov–Smirnov.

Distributions and estimation Methods	Sungai Pahang, Temerloh	Sungai Lipis, Benta
GEV L-moment	**0.139**	**0.133**
GLO L-moment	**0.139**	**0.139**
GPA L-moment	0.009	0.009
GEV TL-moment (1;0)	**0.139**	**0.136**
GLO TL-moment (1;0)	**0.139**	**0.139**
GPA TL-moment (1;0)	0.015	0.022
GEV TL-moment (2;0)	**0.139**	**0.139**
GLO TL-moment (2;0)	**0.139**	**0.139**
GPA TL-moment (2;0)	0.022	**0.052**
GEV TL-moment (3;0)	**0.139**	**0.139**
GLO TL-moment (3;0)	**0.139**	**0.139**
GPA TL-moment (3;0)	0.033	**0.082**
GEV TL-moment (4;0)	**0.139**	**0.139**
GLO TL-moment (4;0)	**0.139**	**0.139**
GPA TL-moment (4;0)	0.045	**0.104**

the significance value, α which means that there is enough evidence to conclude that the probability distributions fit the data well.

Table 8 displays the MADI for the probability distributions of Sungai Pahang and Sungai Lipis. The distribution with the smallest MADI is chosen as the best distribution for each river station. For Sungai Pahang at Temerloh, the GEV with TL-moment $(1,0)$ was found to have the smallest MADI, while for Sungai Lipis at Benta, the GLO with TL-moment $(1,0)$ had the smallest MADI, making it the best distribution. This finding is consistent with that of [7, 32, 33], who discovered that GEV and GLO were appropriate probability distributions for understanding extreme flood events. From Table 8, it is evident that different TL-moment models fit well at different locations. For example, at the Sungai Pahang station, TL-moment $(1,0)$ handles extremes more robustly, while TL-moments $(2,0)$, $(3,0)$, and $(4,0)$ better capture the bulk of the distribution. These results suggest that the variation in the performance of TL-moment models across locations arises from the distinct hydrological and statistical characteristics of each station. Additionally, TL-moment models, which emphasize specific parts of the distribution, are sensitive to factors such as variability, extremes, and skewness. Locations with differing flood regimes, influenced by factors such as climate, topography and catchment characteristics, may exhibit varying levels of outliers or extreme events.

From the Figure 1, it can be said that by using L-moment, Sungai Pahang is better described with GEV distribution when using L-moment method as it has a point the is closer to the GEV distribution

Table 8. MADI for probability distributions of Sungai Pahang, Temerloh and Sungai Lipis, Benta.

Distributions and Estimation Methods	Training Data	Testing Data
GEV L-moment	0.001353	0.001223
GLO L-moment	0.001364	0.000984
GPA L-moment	0.005599	0.002477
GEV TL-moment (1;0)	**0.001278**	0.001498
GLO TL-moment (1;0)	0.001392	**0.000979**
GPA TL-moment (1;0)	0.004262	0.002571
GEV TL-moment (2;0)	0.001435	0.001945
GLO TL-moment (2;0)	0.001543	0.001162
GPA TL-moment (2;0)	0.004656	0.002949
GEV TL-moment (3;0)	0.001703	0.002327
GLO TL-moment (3;0)	0.001754	0.001518
GPA TL-moment (3;0)	0.005241	0.003281
GEV TL-moment (4;0)	0.001986	0.002625
GLO TL-moment (4;0)	0.001956	0.001795
GPA TL-moment (4;0)	0.005829	0.003571

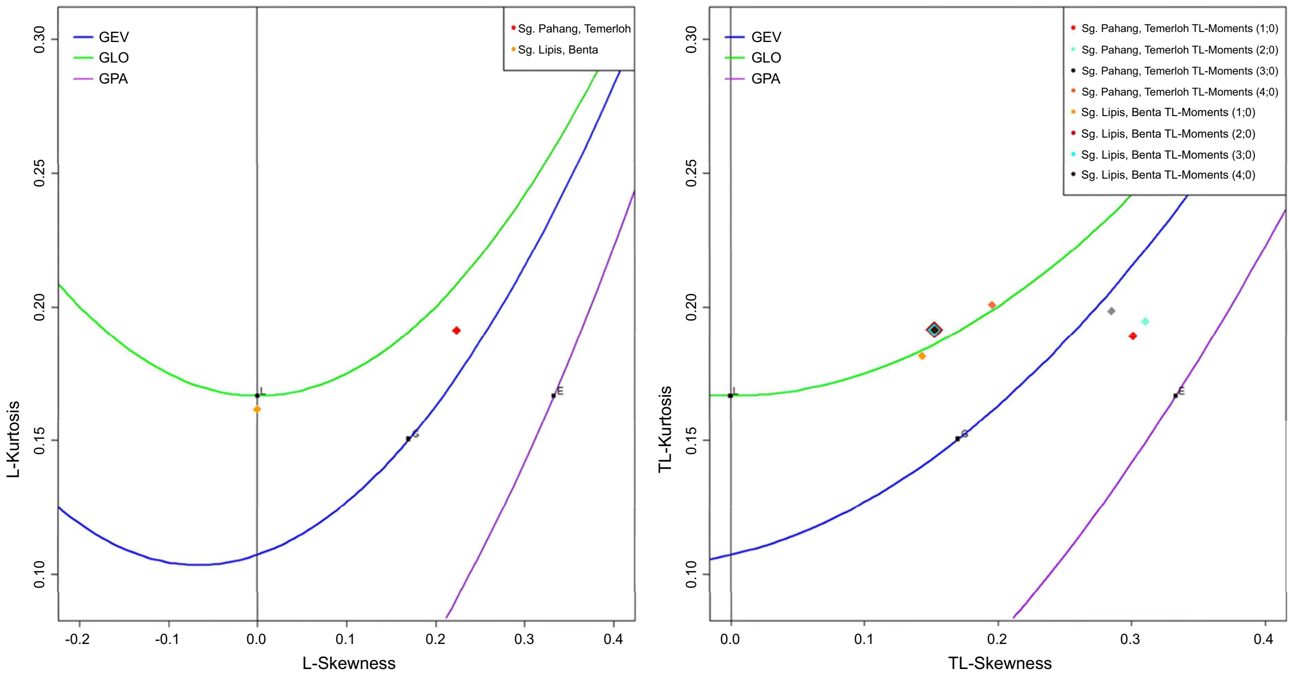

Fig. 1. L-moment and TL-moment ratio diagram.

line as compared to the other two distributions. Meanwhile, the better fit for Sungai Lipis is the GLO distribution as seen in this diagram. This is further supported by the previous MADI where among the L-moment method, Sungai Pahang has GEV as the lowest MADI while Sungai Lipis has GLO as the lowest MADI. Meanwhile for TL-moment, the five points scattered near the GLO distribution line are the TL-moment $(1,2,3,4;0)$ for Sungai Lipis and TL-moment $(4;0)$ for Sungai Pahang. This means that, for these five methods, GLO is more fit for the data. Meanwhile the remaining three methods are scattered near the GEV distribution line. Both datasets were partitioned into 70% training set and 30% testing set from a total of 13 380 water level data for Sungai Pahang, Temerloh and 13 882 water level data for Sungai Lipis, Benta. After partitioning, parameter estimations of the three probability distributions, GEV, GLO, and GPA using L-moment and TL-moment $(1,2,3,4;0)$ were done to both training and testing set for the two river stations. The criterion for selection is determined by comparing their respective error measures by utilizing MADI which can be seen in Table 9 for Sungai Pahang, Temerloh and Table 10 for Sungai Lipis, Benta. The best model is chosen when it has the least value of MADI. GEV TL-moment $(1;0)$ appeared to be the best distribution for Sungai Pahang, Temerloh since it has the smallest value of MADI as compared to other distributions for both training and testing set. Hence, it can be said that GEV is the best fit for the daily water level data of Sungai Pahang, Temerloh river station since it is aligned with the result from the actual data.

Table 9. MADI for Probability Distributions of Sungai Pahang, Temerloh.

Distributions and Estimation Methods	Training Data	Testing Data
GEV L-moment	0.001332	0.01913
GLO L-moment	0.001773	0.01884
GPA L-moment	0.005338	0.02028
GEV TL-moment (1;0)	**0.001178**	**0.01717**
GLO TL-moment (1;0)	0.001748	0.01850
GPA TL-moment (1;0)	0.004027	0.02094
GEV TL-moment (2;0)	0.001197	0.01722
GLO TL-moment (2;0)	0.001893	0.01796
GPA TL-moment (2;0)	0.004321	0.02179
GEV TL-moment (3;0)	0.001271	0.01959
GLO TL-moment (3;0)	0.002289	0.01755
GPA TL-moment (3;0)	0.004782	0.02265
GEV TL-moment (4;0)	0.001407	0.01978
GLO TL-moment (4;0)	0.002688	0.01942
GPA TL-moment (4;0)	0.005260	0.02341

Table 10. MADI for Probability Distributions of Sungai Lipis, Benta.

Distributions and Estimation Methods	Training Data	Testing Data
GEV L-moment	0.0009146	0.01721
GLO L-moment	0.0004840	0.01715
GPA L-moment	0.0019094	0.01735
GEV TL-moment (1;0)	0.0006841	0.01745
GLO TL-moment (1;0)	0.0004536	0.01727
GPA TL-moment (1;0)	0.0012855	0.01776
GEV TL-moment (2;0)	0.0006779	0.01763
GLO TL-moment (2;0)	0.0004619	0.01731
GPA TL-moment (2;0)	0.0012687	0.01808
GEV TL-moment (3;0)	0.0007042	0.01771
GLO TL-moment (3;0)	0.0004518	0.01725
GPA TL-moment (3;0)	0.0013544	0.01829
GEV TL-moment (4;0)	0.0007286	0.01775
GLO TL-moment (4;0)	**0.0004484**	**0.01714**
GPA TL-moment (4;0)	0.0014703	0.01845

Meanwhile, based on Table 10, Sungai Lipis station has GLO with TL-moment $(4;0)$ as the best distribution that best fit the daily water level data. However, for further analysis, for Sungai Lipis station GLO with TL-moment $(1;0)$ will be used since based on the TL-moment Ratio Diagram, it is closer to the GLO distribution line as compared to TL-moment $(4;0)$.

Table 11. Quantile estimates for best fit probability distribution.

Station and distribution	Quantile estimates
(Sg Pahang) GEV [TL-moment(1;0)]	$25.0100+\frac{0.8310}{-0.1043}[1-(-\log[1-\frac{1}{Tx365}])^{-0-1043}$
(Sg Lipis) GLO [TL-moment(1;0)]	$71.1791+\frac{0.5064}{0.0062}[1-([Tx365]-1)^{-0.0062}]$

Table 12. Return period for the river stations.

Years	Sungai Pahang, Temerloh	Sungai Lipis, Benta
2	32.8890	74.4498
5	34.4789	74.8944
10	35.7864	75.2289
50	39.2126	75.9997
100	40.8748	76.3293

The return period for 2, 5, 10, 50, and 100 years of Sungai Pahang, Temerloh and Sungai Lipis, Benta can be seen in Table 12. These values represent the water levels (m) that are expected to be exceeded, on average, once in the specified return period. For Sungai Pahang, Temerloh, it can be said that on average, the water level in Sungai Pahang, Temerloh is expected to exceed 32.8890 m, 34.4789 m, 35.7864 m, 39.2126 m, and 40.8747 m approximately at least once for every 2, 5, 10, 50, and 100 years respectively. Meanwhile, for Sungai Lipis, Benta, the water level is expected to exceed 74.4498 m, 74.8944 m, 75.2289 m, 75.9997 m, and 76.3293 m at least once for every 2, 5, 10, 50, and 100 years respectively. The danger water level for Sungai Pahang, Temerloh and Sungai Lipis, Benta are at 33 m and 75 m respectively. it can be said that the water level is expected to exceed 33 meters for return periods of 5 years, 10 years, 50 years, and 100 years for Sungai Pahang, Temerloh. In other words, the probability of a flood with a water level greater than 33 m increases with longer return periods. Meanwhile, the water level is expected to exceed 75 m for return periods of 10 years, 50 years and 100 years for Sungai Lipis, Benta.

4. Conclusion

This study sought to identify the most suitable probability distributions for predicting extreme water levels at the Sungai Pahang, Temerloh, and Sungai Lipis Benta river stations, using advanced methods such as L-moment and TL-moment. We specifically examined the generalized extreme value (GEV), generalized logistic (GLO), and generalized Pareto (GPA) distributions. Our analysis, guided by Mean Absolute Deviation Index (MADI) and ratio diagrams, identified the GEV TL-moment (1;0) distribution as the most accurate for Sungai Pahang and Temerloh, while the GLO TL-moment (1;0) distribution was best suited for Sungai Lipis and Benta. These findings provide a robust framework for future water level predictions across various return periods (2, 5, 10, 50, 100 years). The results indicate that extreme water levels are likely to exceed danger thresholds for various return periods, underscoring the importance of selecting appropriate distribution models to safeguard communities near these river stations. However, the study's applicability to other regions may be limited by local hydrological and environmental factors. Future research should focus on refining these models with updated data beyond 2009, taking into account the effects of urbanization and climate change on river behavior.

Additionally, while the study provides valuable insights for flood frequency analysis, it is crucial to address the limitations of the current data set, including potential gaps and biases that may affect the results. Enhanced data quality and availability will be essential for more accurate and reliable predictions. The findings also highlight the need for integrating flood frequency analysis with socio-economic factors, urban planning, and engineering design to develop comprehensive flood risk management strategies. To ensure the relevance and effectiveness of flood risk management, it is recommended that a dynamic framework for continuous monitoring and updating be implemented. This should involve regular re-evaluation of models using new data and incorporating feedback from stakeholders to adapt to evolving flood risks. By fostering collaboration between researchers, policymakers, and engineers, we can enhance our ability to mitigate flood risks and promote environmental sustainability. The study's contributions pave the way for more adaptive and resilient flood management practices, benefiting communities and infrastructure both locally and globally.

Acknowledgements

This research was funded by a grant from Universiti Sains Malaysia
(Short Term Grant 304.PMATHS.6315718).

[1] Tekolla A. Rainfall and Flood Frequency Analysis in Pahang River Basin, Malaysia. TVVR10/5012 (2010).

[2] Badyalina B., Mokhtar N. A., Mat Jan N. A., Marsani M. F., Ramli M. F., Majid M., Ya'acob F. F. Hydroclimatic Data Prediction Using a New Ensemble Group Method of Data Handling Coupled with Artificial Bee Colony Algorithm. Sains Malaysiana. **51** (8), 2655–2668 (2022).

[3] Ni C., Marsani M. F., Shan F. P. Flood Prediction Based on Feature Selection and a Hybrid Deep Learning Network. Journal of Water and Climate Change. **15** (3), 1245–1261 (2024).

[4] Ni C., Marsani M. F., Fam P. S., Zou X. Flood prediction with optimized gated recurrent unit-temporal convolutional network and improved KDE error estimation. AIMS Mathematics. **9** (6), 14681–14696 (2024).

[5] Someetheram V., Marsani M. F., Mohd Kasihmuddin M. S., Mohd Jamaludin S. Z., Mansor M. A. Double Decomposition with Enhanced Least-Squares Support Vector Machine to Predict Water Level. Journal of Water and Climate Change. **15** (6), 2582–2594 (2024).

[6] Vinet F. Geographical analysis of damage due to flash floods in southern France: The cases of 12–13 November 1999 and 8–9 September 2002. Applied Geography. **28** (4), 323–336 (2008).

[7] Badyalina B., Mokhtar N. A., Mat Jan N. A., Hassim N. H., Yusop H. Flood Frequency Analysis Using L-Moment for Segamat River. Matematika. **37** (2), 47–62 (2021).

[8] Jan N. A., Marsani M. F., Thiruchelvam L., Abidin N. B. Z., Shabri A., Sani S. A. A. Mitigating infectious disease risks through non-stationary flood frequency analysis: a case study in Malaysia based on natural disaster reduction strategy. Geospatial Health. **18** (2), 1236 (2023).

[9] Ni C., Fam P. S., Marsani M. F. A Data–Driven Method and Hybrid Deep Learning Model for Flood Risk Prediction. International Journal of Intelligent Systems. **2024** (1), 3562709 (2024).

[10] Shabri A. B., Daud Z. M., Mohd Ariff N. Regional analysis of annual maximum rainfall using TL-moments method. Theoretical and Applied Climatology. **104** (3–4), 561–570 (2011).

[11] Ahmad I., Ahmad T., Shahzad U., Ameer M. A., Emam W., Tashkandy Y., Badar Z. Estimation of regional and at-site quantiles of extreme winds under flood index procedure. Heliyon. **10** (1), e23388 (2024).

[12] Mat Jan N. A., Shabri A., Azuardi S. D. TL-Moments: Application to the Generalized Logistic Distribution. Proceedings of the International Conference on Science, Technology and Social Sciences (ICSTSS) 2012. 525–531 (2014).

[13] Anghel C. G., Ilinca C. Predicting Future Flood Risks in the Face of Climate Change: A Frequency Analysis Perspective. Water. **15** (22), 3883 (2023).

[14] Du H., Xia J., Zeng S., Tu Y. Climate Change and Multi-Reservoirs Impacts on Extreme Flood: Nonstationary Regional Frequency Analysis and Uncertainty Estimation. Water Resources Management. **38** (3), 951–965 (2024).

[15] Ilinca C., Stanca S. C., Anghel C. G. Assessing Flood Risk: LH-Moments Method and Univariate Probability Distributions in Flood Frequency Analysis. Water. **15** (19), 3510 (2023).

[16] Khan Z., Rahman A., Karim F. An Assessment of Uncertainties in Flood Frequency Estimation Using Bootstrapping and Monte Carlo Simulation. Hydrology. **10** (1), 18 (2023).

[17] Prahadchai T., Busababodhin P., Parka J.-S. Regional Flood Frequency Analysis of Extreme Rainfall in Thailand, Based on *L*-Moments. Communications for Statistical Applications and Methods. **31** (1), 37–53 (2024).

[18] Vidrio-Sahagún C. T., He J., Pietroniro A. Nonstationary hydrological frequency analysis using the Metastatistical extreme value distribution. Advances in Water Resources. **176**, 104460 (2023).

[19] Vidrio-Sahagún C. T., He J., Pietroniro A. Multi-distribution regula-falsi profile likelihood method for nonstationary hydrological frequency analysis. Stochastic Environmental Research and Risk Assessment. **38** (3), 843–867 (2024).

[20] Hosking J. R. M., Wallis J. R. Regional Frequency Analysis. Cambridge University Press (1997).

[21] Tao D. Q., Nguyen V.-T.-V., Bourque A. On Selection of Probability Distributions for Representing Extreme Precipitations in Southern Quebec. Annual Conference of the Canadian Society for Civil Engineering. **5**, 1–8 (2002).

[22] Abdulali B. A. A., Abu Bakar M. A., Ibrahim K., Ariff N. M. Extreme Value Distributions: An Overview of Estimation and Simulation. Journal of Probability and Statistics. **2022** (1), 5449751 (2022).

[23] Hamed K. H., Rao A. R. A Modified Mann-Kendall Trend Test for Autocorrelated Data. Journal of Hydrology. **204** (1–4), 182–196 (1998).

[24] Hosking J. R. M. L-Moments: Analysis and Estimation of Distributions Using Linear Combinations of Order Statistics. Journal of the Royal Statistical Society, Series B (Methodological). **52** (1), 105–124 (1990).

[25] Elamir E. A. H., Seheult A. H. Trimmed L-Moments. Computational Statistics & Data Analysis. **43** (3), 299–314 (2003).

[26] Shiryaev A. N. Kolmogorov: Life and Creative Activities. The Annals of Probability. **17** (3), 866–944 (1989).

[27] Marsani M. F., Someetheram V., Mohd Kasihmuddin M. S., Mohd Jamaludin S. Z., Mansor M. A., Badyalina B., Mat Jan N. A. Enhancing rainfall prediction in SVM by incorporating the autocorrelation function (ACF). AIP Conference Proceedings. **3123** (1), 70006 (2024).

[28] Marsani M. F., Someetheram V., Mohd Kasihmuddin M. S., Mohd Jamaludin S. Z., Mansor M. A., Badyalina B. The application of seasonal autoregressive integrated moving average (SARIMA) model in forecasting Malaysia mean sea level. AIP Conference Proceedings. **3123** (1), 70005 (2024).

[29] Tehrany M. S., Jones S., Shabani F. Identifying the essential flood conditioning factors for flood prone area mapping using machine learning techniques. CATENA. **175**, 174–192 (2019).

[30] Rao A. R., Hamed H. K. Flood Frequency Analysis. CRC Press (2000).

[31] Tolikas K. Unexpected tails in risk measurement: Some international evidence. Journal of Banking & Finance. **40**, 476–493 (2014).

[32] Ahmad U. N., Shabri A., Zakaria Z. A. Flood Frequency Analysis of Annual Maximum Stream Flows Using L-Moments and TL-Moments Approach. Applied Mathematical Sciences. **5** (5), 243–253 (2011).

[33] Mat Jan N. A., Shabri A., Samsudin R. Handling non-stationary flood frequency analysis using TL-moments approach for estimation parameter. Journal of Water & Climate Change. **11** (4), 966–979 (2020).

Аналіз частоти повеней за рівнем води із застосуванням підходів L-моментів та TL-моментів на річкових станціях у Пахангу

Арба Ф. А. Н.[1], Азахар А. А.[1], Марсані М. Ф.[1], Касіхмуддін М. С. М.[1], Сометехрам В.[1], Мансор М. А.[2], Ян Н. А. М.[3], Джамалудін С. З. М.[1]

[1]*Школа математичних наук, Університет науки Малайзії, 11800 USM, Пенанг, Малайзія*
[2]*Школа дистанційної освіти, Університет науки Малайзії, 11800 USM, Пенанг, Малайзія*
[3]*Кафедра фізико-математичних наук, Факультет природничих наук, Університет Тунку Абдул Рахман, Кампар Кампус, 31900 Кампар, Перак, Малайзія*

Застосування аналізу частоти повеней має важливе значення для розуміння та управління ризиками, пов'язаними з екстремальними рівнями води. У цьому дослідженні розглядається басейн ріки Паханг, особливо зосереджуючись на рівнях води в Сунгай Паханг (Темерлох) і Сунгай Ліпіс (Бента). Для оцінки випадків повеней застосовуються розподіли ймовірностей і поняття періоду повторюваності. Дослідження має дві основні цілі: по-перше, визначити найбільш підходящий розподіл ймовірностей для моделювання повені серед розподілів узагальнених екстремальних значень (GEV), узагальнених логістичних розподілів (GLO) та узагальнених розподілів Парето (GPA), використовуючи як L-моменти, так і TL-моменти для оцінки параметрів; і по-друге, щоб оцінити очікувані рівні води для періодів повторюваності 2, 5, 10, 50 і 100 років, використовуючи визначені найкращі розподіли. Для досягнення цих цілей у дослідженні використовувалися інструменти індексу середнього абсолютного відхилення (MADI) та діаграми співвідношення для оцінки ефективності розподілу. Результати показали, що розподіл GLO, оцінений із застосуванням TL-моментів (1;0), найточніше відповідає даним рівня води. Отримані результати свідчать про те, що рівень води в Сунгай Паханг і Сунгай Ліпіс, ймовірно, перевищить критичні пороги небезпеки в 33 метри та 75 метрів протягом наступних 5 та 10 років відповідно, що підкреслює необхідність проактивних стратегій боротьби з повенями.

Ключові слова: *аналіз частоти паводків; L-моменти; TL-моменти; узагальнений логістичний розподіл; період повторюваності; басейн річки Паханг.*